arXiv:1511.03628v2 [physics.comp-ph] 24 Nov 2015

Computing optimal interfacial structure of ordered phases

Jie Xu[1], Chu Wang[2], An-Chang Shi[3] and Pingwen Zhang[1*]

[1]LMAM & School of Mathematical Sciences, Peking University, Beijing 100871, China
[2]Program in Applied and Computational Mathematics, Princeton University,
Princeton, New Jersey 08544, USA
[3]Department of Physics and Astronomy, McMaster University,
Hamilton, Ontario L8S4M1, Canada
Email: rxj_2004@126.com, chuw@math.princeton.edu, shi@mcmaster.ca, pzhang@pku.edu.cn

November 25, 2015

Abstract

We propose a general framework of computing interfacial structure. If ordered phases are involved, the interfacial structure can be obtained by simply minimizing the free energy with compatible boundary conditions. The framework is applied to Landau-Brazovskii model and works efficiently.

Keywords: Interface; Ordered phase; Metastable state; Boundary compatibility; Landau-Brazovskii model.

1 Introduction

Interfaces are transition regions between two different materials, two different phases of the same material, or two grains of the same phase with different orientations (grain boundaries). Being less stable, interfacial regions are where most of the molecular motion takes place. Therefore, the morphology of interfaces greatly affects the mechanical, thermal and electrical properties of the material. Interfaces are frequently encountered as planar defects and in phase transitions. In specific, the strength and conductivity of the material depend hugely on the distribution and morphology of grain boundaries. And in first-order phase transitions, the interfacial properties play an important role in the nucleation-growth process.

In the framework of mean-field theory, the majority of literatures on interfaces are dedicated to grain boundaries, among which, two distinct approaches are usually adopted. One approach, which could be summarized as the dynamical approach, treats the interface as a transient state and focuses on its dynamics. It has been adopted to examine grain boundaries of lamellar and cylindral phases [1, 2, 3]. The other regards the interface as a metastable state and its morphology is considered as a local minimizer of system's energy under some conditions. It has been adopted to investigate a few tilted grain boundaries of the lamellar phase [4, 5, 6, 7] and the bcc phase [8], and twist grain boundaries of several cubic phases [9].

*Corresponding author

The dynamical approach enables us to see the dynamical evolution of the interface, and is especially useful when we are interested in how several grains interact with each other. But it is difficult to reach full relaxation. Even if only partial relaxation is required, the simulation is more time-consuming because of the stability condition. The minimization approach, on the other hand, is able to reach full relaxation and reveal clearly the structure. Furthermore, fast optimization algorithms can be used in the computation. Since we aim to analyze the structural properties of interfaces, the minimization approach appears the better way.

Because the interface is away from equilibrium, a delicate handling of the boundary conditions is required. If the boundary conditions are incompatible with each grain, a large cell is needed to reduce the boundary effect, for the incompatibility might destroy the structure inside the grain. Despite the possibility of only finding inaccurate or even biased structures, incompatible boundary conditions are adopted in most relevant works. In addition, they may generate several interfaces (Fig. 5.20 in [10] gives a typical morphology) or may not work at all (see the examples in [2]). From another perspective, compatible boundary conditions can sufficiently reduce the size of the computational cell. The compatibility has been noted in the study of kink [5] and T-junctions [7] in lamellar grain boundaries, where the basis functions are carefully chosen to retain symmetry properties. However, the compatibility is only partially reached, and the choice of basis functions cannot be easily extended to other structures. Thus it is desirable to propose boundary conditions with universal compatibility.

In contrast to grain boundaries, few theoretical works report the morphology of interfaces between different phases. Some works construct the interface profile by a mixing ansatz, which is the direct weighted combination of two bulk phase profiles:

$$\phi(x) = (1 - \alpha(x))\phi_1(x) + \alpha(x)\phi_2(x) \tag{1}$$

where $\phi_k(x)$ are profiles of two bulk phases, and $\alpha(x)$ is a smooth monotone function satisfying $\alpha(-\infty) = 0,\ \alpha(+\infty) = 1$. This method proves to be convenient and effective in several literatures [11, 12]. But this artificial approach may exclude the possibility of complex interfacial structures as we will present later. To our best knowledge, only in [4] the morphology of a few lamellar-cylindral interfaces is reported.

When considering interfaces between different phases, there is another question to care about: can we pose it purely as an energy minimization problem? Intuitively, the phase with higher energy density will gradually be taken over by the other phase. We may try to choose parameters to equalize the energy densities, but it is difficult to realize in computation. Thus it seems that constraints are needed to prevent the interface from moving continuously towards the less stable phase. However, we will show in this paper that constraints of such kind are not necessary if the bulk phases are ordered. The interface will be stuck at a locally optimized position even if the energy densities of the two phases are slightly different. Thus we may let the interface freely relax itself during the computation instead of intervening in the process artificially.

To sum up, we are going to propose a general framework for the computation of interfacial structures. In this framework, optimization approach is adopted to inherit the advantage of full relaxation of the system and fast optimization methods. The boundary conditions, or equivalently the choice of function spaces, are compatible with two bulk phases. The setting is well-posed for ordered phases with energy difference. We will apply this framework to Landau-Brazovskii model to illustrate the above features. The paper is organized as follows. In Sec. 2, the general framework of interface problem is described, and the well-posedness of

the setup is illustrated. Some interfacial structures in Landau-Brazovskii model are presented in Sec. 3. Finally we summarize the paper in Sec. 4. Some details of numerical method are written in Appendix.

2 General framework

2.1 Boundary compatibility

When considering an interface between two ordered structures, their spatial and orientational relations are essential variables. Let us put the two phases in two half-spaces separated by the plane $x = 0$. Denote the two phases by α and β respectively. Both phases can be rotated or shifted, represented by orthogonal matrices $\mathcal{R}_\alpha$, $\mathcal{R}_\beta$, and vectors $\boldsymbol{d}_\alpha$, $\boldsymbol{d}_\beta$. Each of these four quantities has three degrees of freedom. Note that their relative position remains unchanged if they are rotated together round the x-axis or shifted together in the y-z plane, so there are nine independent degrees of freedom in total.

Assume that the density profile of a phase can be expressed by a single function ϕ. More specifically, we assume that the phase is periodic. In this case, the profile is given by the value of ϕ in a unit cell, which can be written as

$$\phi(\boldsymbol{r}) = \sum_{\boldsymbol{k}\in\mathbb{Z}^3} \phi_{\boldsymbol{k}} \exp\left(i \sum_{j=1}^{3} k_j \boldsymbol{b}_j \cdot \boldsymbol{r} \right). \tag{2}$$

If the phase is rotated by $\mathcal{R}$, then shifted by $\boldsymbol{d}$, the profile becomes

$$\phi(\boldsymbol{r}; \mathcal{R}, \boldsymbol{d}) = \phi(\mathcal{R}^T(\boldsymbol{r} - \boldsymbol{d})) = \sum_{\boldsymbol{k}\in\mathbb{Z}^3} \phi_{\boldsymbol{k}} \lambda_{\boldsymbol{k}} \exp\left(i \sum_{j=1}^{3} k_j (\mathcal{R}\boldsymbol{b}_j) \cdot \boldsymbol{r} \right), \tag{3}$$

where $\lambda_{\boldsymbol{k}} = \exp(-i \sum_{j=1}^{3} k_j \boldsymbol{d}^T \mathcal{R} \boldsymbol{b}_j)$.

Now let us explain what is compatibility. Suppose that two phases α and β are identical. In this case, the whole space is filled with the phase α and no interface exists. The boundary conditions we propose shall not damage the structure of α and generate an interface artificially. In other words, the boundary conditions shall be met by the profile ϕ_α as well as ϕ_β. Equivalently, from the view of function space, it requires that the basis functions we choose shall contain that of ϕ_α and ϕ_β.

We apply the compatibility to the y- and z-directions. Consider the limitation of ϕ onto the plane $x = x_0$. Denote $\boldsymbol{r}' = (y, z)$. Then we have

$$\phi_\alpha(x_0, \boldsymbol{r}'; \mathcal{R}_\alpha, \boldsymbol{d}_\alpha) = \sum_{\boldsymbol{k}\in\mathbb{Z}^3} \phi_{\alpha\boldsymbol{k}} \tilde{\lambda}_{\alpha\boldsymbol{k}} \exp\left(i \sum_{j=1}^{3} k_j \boldsymbol{b}'_{\alpha j}(\mathcal{R}_\alpha) \cdot \boldsymbol{r}' \right),$$

where $\boldsymbol{b}'_{\alpha j}(\mathcal{R}_\alpha)$ denotes the y and z components of $\mathcal{R}_\alpha \boldsymbol{b}_{\alpha j}$, and $\tilde{\lambda}_{\alpha\boldsymbol{k}} = \lambda_{\alpha\boldsymbol{k}} \exp\left(i x_0 \sum_{j=1}^{3} k_j (\mathcal{R}_\alpha \boldsymbol{b}'_{\alpha j})_1 \right)$. It becomes a quasiperiodic function in the plane. And for ϕ_β, we have

$$\phi_\beta(x_0, \boldsymbol{r}'; \mathcal{R}_\beta, \boldsymbol{d}_\beta) = \sum_{\boldsymbol{k}\in\mathbb{Z}^3} \phi_{\beta\boldsymbol{k}} \tilde{\lambda}_{\beta\boldsymbol{k}} \exp\left(i \sum_{j=1}^{3} k_j \boldsymbol{b}'_{\beta j}(\mathcal{R}_\beta) \cdot \boldsymbol{r}' \right).$$

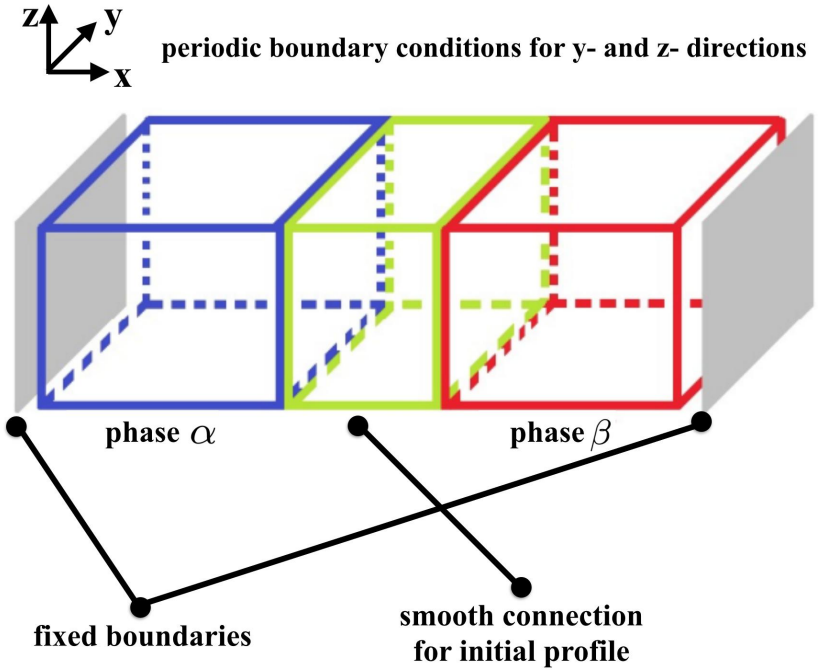

Fig. 1: Schematic of the setting of interface problem.

Then a natural choice will be the set of quasiperiodic function

$$\mathcal{F} = \left\{ f(\boldsymbol{r}') : f(\boldsymbol{r}') = \sum_{\boldsymbol{k},\boldsymbol{l}\in\mathbb{Z}^3} f_{\boldsymbol{k}} \exp\left(i \sum_{j=1}^{3} \left(k_j \boldsymbol{b}'_{\alpha j}(\mathcal{R}_\alpha) + l_j \boldsymbol{b}'_{\beta j}(\mathcal{R}_\beta) \right) \cdot \boldsymbol{r}' \right) \right\}. \tag{4}$$

Actually, this choice is also valid if ϕ is quasiperiodic, namely to substitute the sum over $1 \le j \le 3$ with $1 \le j \le m$. In special cases where $k_j \boldsymbol{b}'_{\alpha j}(\mathcal{R}_\alpha) + l_j \boldsymbol{b}'_{\beta j}(\mathcal{R}_\beta)$ lie on a 2D lattice, $\mathcal{F}$ is reduced to a set of periodic functions, indicating that two phases, with their relative position determined, have public period in the y-z plane. The current work will focus on these special cases.

In the x-direction, we select a length L and set ϕ outside $[-L, L]$ equal to the bulk value. Here L is large enough to contain the transition region. Such setting will induce some anchoring conditions at $x = \pm L$ dependent on the energy functional. If Laudau-type energy functional is used, these conditions can usually be determined by smoothness requirements of the density profile ϕ. For example, if ϕ is C^k, then $\phi, \ldots, \nabla^k \phi$ shall be fixed to bulk values at $x = \pm L$. It should be noted that in some other models boundary conditions are not directly imposed on the density profile. For example, in self-consistent field theory (we refer to [10] for details), the profile is calculated through a propagator q, on which boundary conditions are imposed. In this case the anchoring conditions can be used on q.

To initialize the density profile for computation in our frame work, we use the setting in Fig. 1. We first choose a common period in y- and z- direction for phase α and β, and then fill in the bulk profiles and anchor both ends of the region. To obtain a smooth initial value, the density profile in the middle region is set as the convex combination of the bulk densities as in (1).

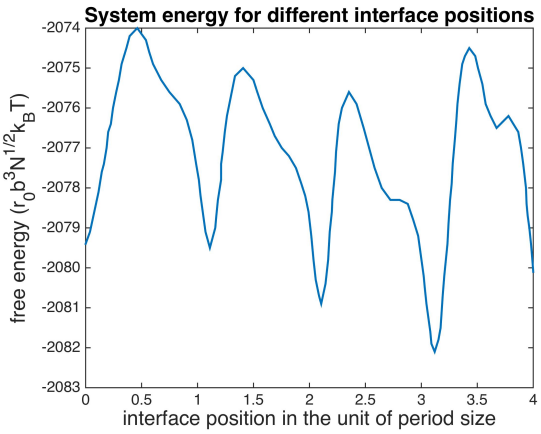

Fig. 2: Energy profile in the movement of cylindral-gyroid interface within a single period. The location of interface is calculated using a modified functional distance between the interfacial density and the two bulk densities [13, 14]. The distance is measured by the unit cell of gyroid, which is rescaled to four (the upper bound of the x-axis).

2.2 Existence of local minima

Before solving the optimization problem, the well-posedness of this setting should be discussed. More specifically, we need to demonstrate the existence of local minima in our setting. It is obvious that for disorder-disorder interface, if there exists a difference in the bulk energy densities, no matter how small it is, the interface would move continuously to the one with higher energy density. In this case, the total energy can be written as

$$E = f_\alpha V_\alpha + f_\beta V_\beta + \gamma S \tag{5}$$

where f is the free energy density, V is the volume of each phase, S is the area of interface, and γ is the interfacial energy density. The isotropy of two phases along the x-direction makes γ independent of interface location. Suppose $f_\alpha < f_\beta$, then E is monotone decreasing when V_α increases, driving the interface to the phase β. In some earlier works on liquid-vapor nucleation, constraint method has been used to fix the location of interface [15, 16, 17]. The constraint acts equivalently as the chemical potential that fixes the volume fraction of each phase. Nevertheless, it is difficult to propose a constraint in ordered systems physically meaningful.

Fortunately, we can benefit from anisotropy in ordered phases. The anisotropy implies that γ is no longer constant. Intuitively we write $\gamma = \gamma(x)$ as a function of interface location, and still write the total energy as (5). If $\gamma(x)$ varies more drastically than the bulk energy difference, some local minima exist, towards which we may let the interface relax. Such condition is easier to be attained when the energy difference between two phases is small. This can be achieved by choosing model parameters near (but not necessarily on) the binodal line. In fact, only when the parameters lie in this range could the interfaces exist. Otherwise the phase of higher energy density will disappear under tiny perturbation, or even become unstable and quickly decompose into the stable phase.

We would like to give an example to illustrate the how the total energy varies as the interface moves. We compute the cylindral-gyroid interfaces in the Landau-Brazovskii model

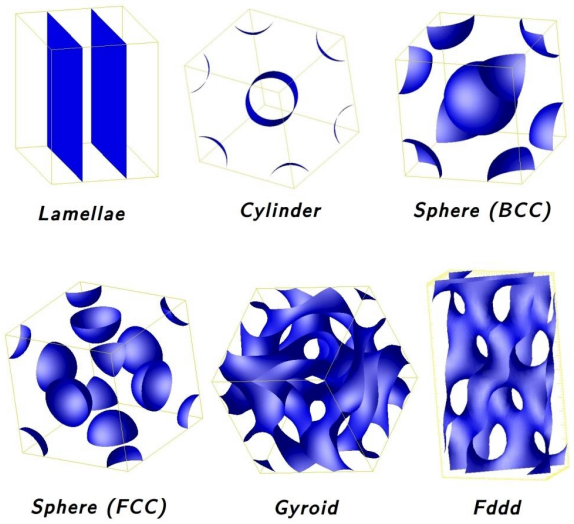

Fig. 3: Bulk phases of Landau-Brazovskii model.

(6) with parameters $\xi^2 = 1.0$, $\tau = -0.3$, $\gamma = 0.383$. Four local minima are found within a single period along the x-direction, and they are connected with the minimum energy path computed using string method [13, 14]. Fig. 2 shows clearly that the energy decreases in a wavy manner as the interface moves. The morphology of interfaces at local minima is identical to what is drawn in Fig. 4 (in which we draw the interfaces within two periods), although we choose different parameters.

As we mentioned in Sec. 1, quite few works examine interfaces between different phases. The reason could be the lack of knowledge of the existence of local minima produced by microstructures. We feel that the clarification of the energy profile would be helpful to the computation of interfacial structure.

3 Application to Landau-Brazovskii model

In this section, we apply our framework for interface to Landau-Brazovskii (LB) model. We first present the cylindral-gyroid and lamellar-gyroid interfaces in epitaxially matching cases, in which the local minima are shown clearly. Furthermore, a few novel examples of non-matching cases are given to show the effectiveness of our framework and algorithm.

3.1 The free energy

LB model was developed to treat fluctuation effects in systems undergoing weak crystallization [18, 19]. This model can be viewed as a generic model for modulated phases occurring in a variety of physical and chemical systems, and its form is similar to many Landau-type free energy functionals for different kinds of materials. In addition, LB model can describe frequently observed patterns in all kinds of modulated systems, including lamellar(L), cylindral(C), spherical and gyroid(G) structures. Therefore our results could reveal properties of interfaces in a wide range of systems. In its scaled form, the LB free energy density is given

by

$$F = \frac{1}{V}\int_{\Omega} \mathrm{d}\boldsymbol{r}\{\frac{\xi^2}{2}[(\nabla^2 + q_0^2)\phi]^2\} + \frac{\tau}{2}\phi^2 - \frac{\gamma}{3!}\phi^3 + \frac{1}{4!}\phi^4, \tag{6}$$

where $q_0 = 1$ is the critical wavelength, ξ, τ, γ are phenomenological parameters, and ϕ is conserved,

$$\int \mathrm{d}\boldsymbol{r}\phi = 0.$$

The parameters can be determined by measurable parameters in some cases. An example is the system of A-B diblock copolymer, in which these parameters are derived from χN and f, where χN is a normalized parameter characterizing the segregation of two blocks, and f is the fraction of block A. The phases in LB model can be easily recognized by the isosurface of ϕ, drawn in Fig. 3. For the interfaces, we will also draw the isosurface to reveal their structures.

3.2 Boundary conditions

Bulk values are needed for setting initial and boundary values of the problem. They are obtained by minimizing (6) with periodic boundary condition in all three directions. The existence of second derivatives in the energy functional requires ϕ and $\nabla\phi$ to be fixed at $x = \pm L$. These values can be easily computed with bulk profiles.

When computing bulk profiles, the period lengths should be optimized as well. This is because the size of the cell also affects the energy density of the system. When two phases coexist, however, it is usually observed experimentally that two unit cells perturb a little from the optimal to match each other [20, 21, 22, 23]. To capture the interfacial structure in our framework, we slightly stretch the two bulks to let them have common period lengths. Then our framework for the interface could be applied directly. Such stretching is feasible since it will affect the energy within a negligibly small amount. It should be pointed out that besides the period matching, different ordered structures have certain preferences in orientation when they coexist, namely the rotations $\mathcal{R}_\alpha$, $\mathcal{R}_\beta$ and the shifts $\boldsymbol{b}_\alpha$, $\boldsymbol{b}_\beta$ prefer certain values. Such epitaxial relationships are also noted in the experimental works mentioned above, and are studied in [12] extensively. We will examine such epitaxies as well as less optimal matching cases for the interfacial systems.

The profiles of L, C and G are calculated with the common period $2\sqrt{6}\pi \times 2\sqrt{6}\pi \times 2\sqrt{6}\pi$, which is almost accurate for lamellar and cylinder, while 4% smaller for gyroid. The number of meshes used in a unit cell is $32 \times 32 \times 32$. Details of discretization and optimization method are given in Appendix, in which acceleration techniques are included.

3.3 C-G and L-G interfaces

We start from the cases in which two phases are epitaxially matched. In the lattice of G, the layer of L parallels to the plane $(11\bar{2})$ and the hexagonal lattice of C lies in the plane (111). The results in Fig. 4 are calculated with $\xi^2 = 0.0389$, $\gamma = 0.0681$; $\tau = -0.0121$ for C-G interfaces and $\tau = -0.0159$ for L-G interfaces. Fig. 4 presents C-G and L-G interfaces at local energy minima. Both C-G and L-G interfaces show four local minima within one period, and when moving a full period, the interfacial structures reappear. We are also able to catch how the interface moves from the ones at discrete locations.

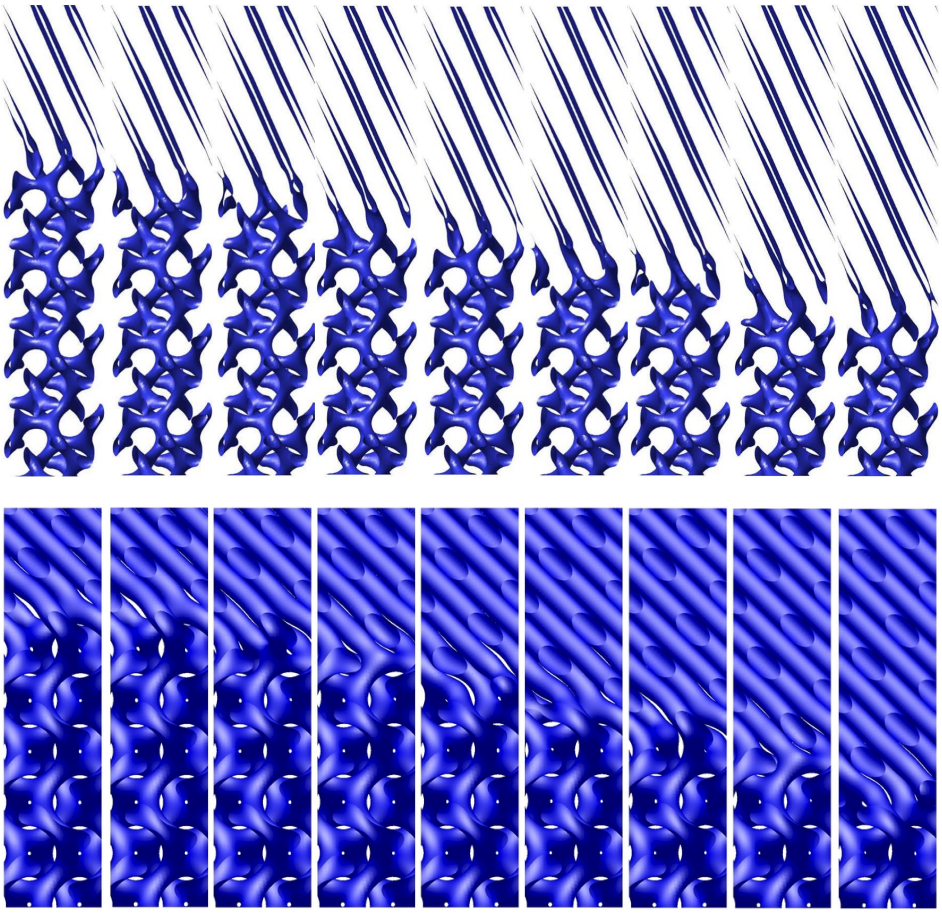

Fig. 4: L-G and C-G interfaces at local minima (within two periods): the epitaxially matching case.

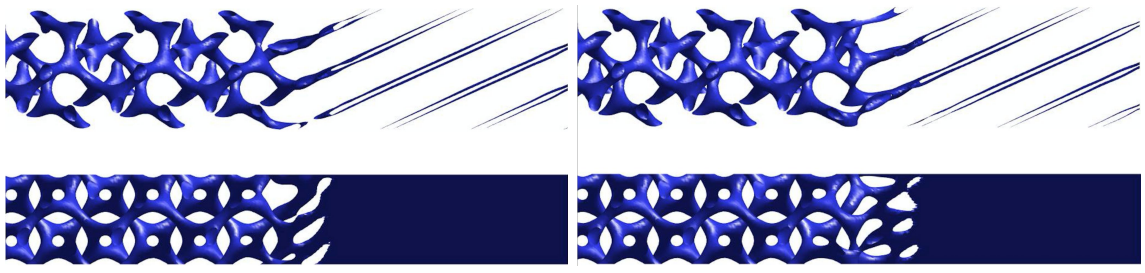

Fig. 5: The L-G interface. Left: the epitaxially matching case; Right: L is shifted a half period. Viewed along the layer of L (upper) and the unit cell of G (lower).

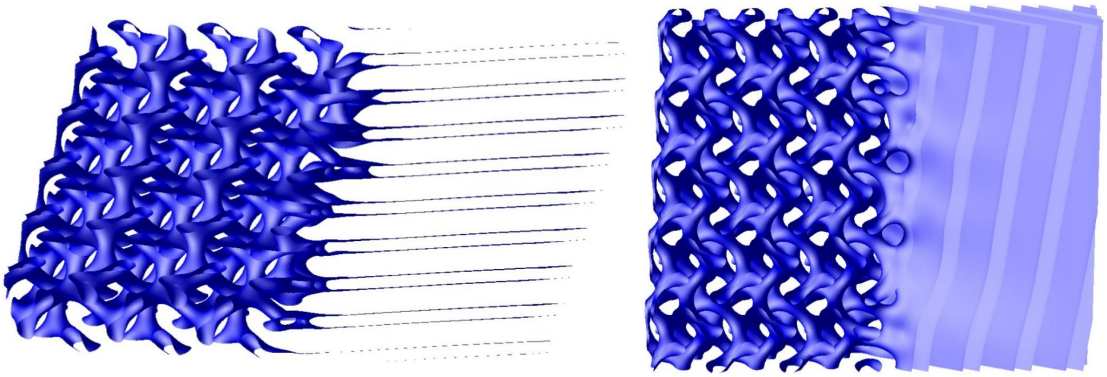

Fig. 6: L-G interfaces with L rotated counter-clockwise $\theta = \arcsin(3/5)$ (left), and $\theta + \pi/2$ (right).

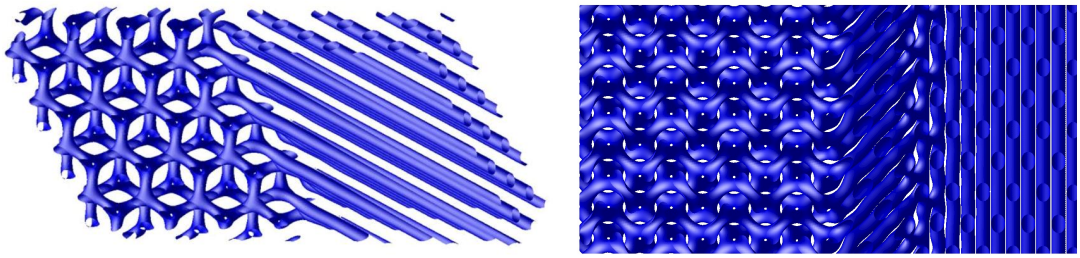

Fig. 7: Left: C-G interface with newly found epitaxy $(1\bar{1}0)$. Right: C is rotated $\pi/2$ from the new epitaxy and cylinder along $\langle 111 \rangle$ direction is found in between.

In the following, we will present some results of the non-matching cases, in which we can observe some interesting phenomena. The results described in this paragraph are calculated with $\xi^2 = 0.0389$, $\gamma = 0.0601$, $\tau = -0.0121$. First, we examine the case where L is shifted a half period (Fig. 5 right). Comparing it with the epitaxially matching case (Fig. 5 left), we find the structure distinct from L and G in the middle. It resembles the metastable perforated layer structure, supporting the prevalent observation of perforated layer phase in the L$\leftrightarrow$G transitions (see the discussion in [24]). Next we look at the effects of relative rotation. In Fig. 6 L is rotated $\theta = \arcsin(3/5)$ and $\theta + \pi/2$ counter-clockwise respectively, G unchanged. Local distortions help to keep their connection, leading to non-planar interfaces.

The next pair of examples are based on the newly-found epitaxially relationship between C and G [23], where the lattice of C is slightly deformed from the regular hexagon and lies in the plane $(1\bar{1}0)$. The parameters are chosen as $\xi^2 = 0.0375$, $\gamma = 0.0757$, $\tau = -0.0102$. The interface is drawn in the left of Fig. 7, which is planar with smooth connection. The right of Fig. 7 shows the interface where C is rotated $\pi/2$ in the x-y plane. To connect two phases, C of the regular hexagonal type with classical epitaxy appears in between.

4 Summary

In this paper, we propose a general framework for computing interfacial structures of ordered phases with optimization approach. In the framework boundary conditions imposed are compatible with both bulk phases. Unlike computing interface between disordered phases where constraints need to be introduced, the problem is well-posed because anistropy leads to local minima that stabilize the location of interface. As an example, we apply the framework to Landau-Brazovskii model. It works efficiently in both epitaxially matching and non-matching cases.

So far we show the application of the framework to special cases where public period can be found in the y-z plane. The choice of basis functions (4) actually allows us to investigate quasiperiodic phases. Thus in the future we aim to apply this framework to broader cases, especially for quasiperiodic phases.

Acknowldegment Pingwen Zhang is partly supported by National Natural Science Foundation of China (Grant No. 11421101, No. 11421110001 and No. 21274005).

A Numerical details

We describe the numerical details of discretization and optimization. For the discretization of density profile, finite difference scheme is adopted in the x-direction. In the y-z plane, both finite difference scheme and Fourier expansion can be used.

In the x-direction, Laplacian is approximated by

$$\partial_x^2\phi(x_k) \approx \delta_x^2\phi(x_k) = \frac{\phi_{k+1} - 2\phi_k + \phi_{k-1}}{\Delta x^2}.$$

The same approximation is adopted when using finite difference scheme in the y-z plane. When using Fourier expansion in the y-z plane, we write ϕ as

$$\phi(x, y, z) = \sum_{\boldsymbol{G}} \phi_{\boldsymbol{G}}(x) \exp(i(\boldsymbol{G} \cdot \boldsymbol{r}')).$$

where $\boldsymbol{G} = m\boldsymbol{b}_1' + n\boldsymbol{b}_2'$, $\quad |m|, |n| \le N$, $\boldsymbol{b}_i'$ are reciprocal vectors with respect to the lattice in the y-z plane, and $\boldsymbol{r}' = (y, z)$. Note that ϕ is real-valued, thus it requires $\phi_{-\boldsymbol{G}}(x) = \phi_{\boldsymbol{G}}^*(x)$.

The anchoring boundary conditions at $x = \pm L$ are implemented by adding two extra grids on each side and setting ϕ equal to bulk values. This can be equivalently viewed as approximating boundary conditions with finite difference scheme,

$$\phi(-L) = \phi_\alpha(-L), \qquad \partial_x\phi(-L) \approx \frac{\phi_0 - \phi_{-1}}{\Delta x} = \frac{\phi_\alpha(x_0) - \phi_\alpha(x_{-1})}{\Delta x} \approx \partial_x\phi_\alpha(-L).$$

The gradient vector can be calculated by

$$\nabla\tilde{F}(\phi(x)) = \xi^2[(\delta_x^2 + \delta_y^2 + \delta_z^2 + 1)^2 + \tau]\phi(x) - \frac{\gamma}{2}\phi^2(x) + \frac{1}{6}\phi^3(x)$$

for finite difference method, and by

$$\nabla\tilde{F}(\phi_{\boldsymbol{G}}(x)) = \xi^2[(\delta_x^2 - \boldsymbol{G}^2 + 1)^2 + \tau]\phi_{\boldsymbol{G}} - \frac{\gamma}{2}\sum_{\boldsymbol{G}_1+\boldsymbol{G}_2=\boldsymbol{G}} \phi_{\boldsymbol{G}_1}\phi_{\boldsymbol{G}_2} + \frac{1}{6}\sum_{\boldsymbol{G}_1+\boldsymbol{G}_2+\boldsymbol{G}_3=\boldsymbol{G}} \phi_{\boldsymbol{G}_1}\phi_{\boldsymbol{G}_2}\phi_{\boldsymbol{G}_3} \tag{7}$$

for Fourier expansion. The convolution sum can be calculated by FFT.

The conservation of ϕ is attained by a projection on the gradient vector: for finite difference scheme, we use

$$\nabla F(\phi(x)) = \nabla \tilde{F}(\phi(x)) - c;$$

and for Fourier expansion, we use

$$\nabla F(\phi_{\boldsymbol{G}}(x)) = \nabla \tilde{F}(\phi_{\boldsymbol{G}}(x)) - c\delta(\boldsymbol{G} = 0).$$

In the above, c can be determined by the following observation: if we set $\phi = \phi_\alpha$ for $x < 0$ and $\phi = \phi_\beta$ for $x > 0$, the constraint is satisfied. So we can just require

$$\int_S \int_{-L}^{L} \phi \mathrm{d}x\mathrm{d}y\mathrm{d}z = \int_S \mathrm{d}y\mathrm{d}z(\int_{-L}^{0} \phi_\alpha \mathrm{d}x + \int_0^L \phi_\beta \mathrm{d}x) \triangleq c_0.$$

For finite difference scheme, we use a gradient method

$$\phi^{n+1}(x) - \phi^n(x) = -a_n \nabla F(\phi^n(x)).$$

The coefficient a_n is altered adaptively with Barzilai-Borwein method [25, 26]. For Fourier expansion we use a semi-implicit scheme to solve the Euler-Langrange equation (7) with

$$\begin{aligned} \frac{\phi_{\boldsymbol{G}}^{n+1}(x) - \phi_{\boldsymbol{G}}^n(x)}{\Delta t} &= -\xi^2[(\delta_x^2 - \boldsymbol{G}^2 + 1)^2 + \tau]\phi_{\boldsymbol{G}}^{n+1} \\ &\quad + \frac{\gamma}{2} \sum_{\boldsymbol{G}_1 + \boldsymbol{G}_2 = \boldsymbol{G}} \phi_{\boldsymbol{G}_1}^n \phi_{\boldsymbol{G}_2}^n - \frac{1}{6} \sum_{\boldsymbol{G}_1 + \boldsymbol{G}_2 + \boldsymbol{G}_3 = \boldsymbol{G}} \phi_{\boldsymbol{G}_1}^n \phi_{\boldsymbol{G}_2}^n \phi_{\boldsymbol{G}_3}^n \\ &\quad - c\delta(\boldsymbol{G} = 0). \end{aligned}$$

References

[1] K. R. Elder and M. Grant. Modeling elastic and plastic deformations in nonequilibrium processing using phase field crystals. *Phys. Rev. E*, 70:051605, 2004.

[2] A. V. Kyrylyuk and J. G. E. M. Fraaije. Three-Dimensional Structure and Motion of Twist Grain Boundaries in Block Copolymer Melts. *Macromolecules*, 38:8546–8553, 2005.

[3] A. D. Pezzutti, D. A. Vega, and M. A. Villar. Dynamics of dislocations in a two-dimensional block copolymer system with hexagonal symmetry. *Phil. Trans. R. Soc. A*, 369:335–350, 2011.

[4] R. R. Netz, D. Andelman, and M. Schick. Interfaces of Modulated Phases. *Phys. Rev. Lett.*, 79(6):1058–1061, 1997.

[5] M. W. Masten. Kink grain boundaries in a block copolymer lamellar phase. *J. Chem. Phys.*, 107(19):8110–8119, 1997.

[6] Y. Tsori, D. Andelman, and M. Schick. Defects in lamellar diblock copolymers: Chevron- and ω-shaped tilt boundaries. *Phys. Rev. E*, 61(3):2848–2858, 2000.

[7] D. Duque, K. Katsov, and M. Schick. Theory of T junctions and symmetric tilt grain boundaries in pure and mixed polymer systems. *J. Chem. Phys.*, 117(22):10315–10320, 2002.

[8] A. Jaatinen, C. V. Achim, K. R. Elder, and T. Ala-Nissila. Thermodynamics of bcc metals in phase-field-crystal models. *Phys. Rev. E*, 80:031602, 2009.

[9] M. Belushkin and G. Gompper. Twist grain boundaries in cubic surfactant phases. *J. Chem. Phys.*, 130:134712, 2009.

[10] G. H. Fredrickson. *The equilibrium theory of inhomogeneous polymers*. Clarendon Press, Oxford, 2006.

[11] K. Yamada and T. Ohta. Interface between Lamellar and Gyroid Structure in Diblock Copolymer Melts. *Journal of the Physical Society of Japan*, 76(8):084801, 2007.

[12] C. Wang, K. Jiang, P. Zhang, and A. C. Shi. Origin of epitaxies between ordered phases of block copolymers. *Soft Matter*, 7:10552–10555, 2011.

[13] W. E, W. Ren, and E. V. Eijnden. String method for the study of rare events. *Phys. Rev. B*, 66:052301, 2002.

[14] W. E, W. Ren, and E. V. Eijnden. Simplified and improved string method for computing the minimum energy paths in barrier-crossing events. *J. Chem. Phys.*, 126:164103, 2007.

[15] V. Talanquer and D. W. Oxtoby. Dynamical density functional theory of gas-liquid nucleation. *J. Chem. Phys.*, 100(7):5190–5200, 1994.

[16] V. Talanquer and D. W. Oxtoby. Nucleation on a solid substrate: A density-functional approach. *J. Chem. Phys.*, 104(4):1483–1492, 1996.

[17] V. Talanquer and D. W. Oxtoby. Nucleation in a slit pore. *J. Chem. Phys.*, 114(6):2793–2801, 2001.

[18] G. H. Fredrickson and E. Helfand. Fluctuation effects in the theory of microphase separation in block copolymers. *J. Chem. Phys*, 87(1):697–705, 1987.

[19] E. I. Kats, V. V. Lebedev, and A. R. Muratov. Weak crystallization theory. *Physics reports*, 228(1):1–91, 1993.

[20] M. F. Schulz, F. S. Bates, K. Almdal, and K. Mortensen. Epitaxial Relationship for Hexagonal-to-Cubic Phase Transition in a Block Copolymer Mixture. *Phys. Rev. Lett.*, 73(1):86–89, 1994.

[21] D. A. Hajduk, S. M. Gruner, P. Rangarajan, R. A. Register, L. J. Fetters, C. Honeker, R. J. Albalak, and E. L. Thomas. Observation of a Reversible Thermotropic Order-Order Transition in a Diblock Copolymer. *Macromolecules*, 27:490–501, 1994.

[22] J. Bang and T. P. Lodge. Mechanisms and Epitaxial Relationships between Close-Packed and BCC Lattices in Block Copolymer Solutions. *J. Phys. Chem. B*, 107(44):12071–12081, 2003.

[23] H. W. Park, J. Jung, T. Chang, K. Matsunaga, and H. Jinnai. New Epitaxial Phase Transition between DG and HEX in PS-*b*-PI. *J. Am. Chem. Soc*, 131:46–47, 2009.

[24] X. Cheng, L. Lin, W. E, P. Zhang, and A. Shi. Nucleation of Ordered Phases in Block Copolymers. *Phys. Rev. Lett.*, 104:148301, 2010.

[25] J. Barzilai and J. M. Borwein. Two-point step size gradient methods. *IMA J. Numer. Anal.*, 8:141–148, 1988.

[26] B. Zhou, L. Gao, and Y. H. Dai. Gradient Methods with Adaptive Step-Sizes. *Computational Optimization and Applications*, 35:69–86, 2006.